Characterisation of the tin oxide conducting film obtained by ultrasonic spray pyrolysis

Marek Nocuń

Department of Materials Science and Ceramic, University of Mining and Metallurgy, al. Adama Mickiewicza 30, 30–059 Kraków, Poland, and Surface Spectroscopy Laboratory, Joint Centre for Chemical Analysis and Structural Research, Jagiellonian University, ul. Władysława Reymonta 23, 30–059 Kraków, Poland, e-mail: nocun@uci.agh.edu.pl.

Tin oxide thin film was obtained by ultrasonic spray pyrolysis technique on a glass substrate using different precursors ($SnCl_4$, $SnCl_2$, $SnCl_2 \times 2H_2O$). Tin oxide layers were characterised by optical spectroscopy (UV-VIS), photoelectron spectroscopy (XPS), and scanning electron microscopy (SEM) technique. Different precursors used in solution preparation led to differences in morphology, conductivity and growth rate of the tin oxide films.

Keywords: SnO_2, thin film, spray pyrolysis.

1. Introduction

Tin oxide film has been investigated intensively because of its high transmittance in the visible spectral range in combination with a relatively high conductivity. Undoped and doped by various oxides (indium, antimonium, fluorine), tin oxide has a broad application in optic and electronic devices [1]–[3], as a gas sensor [4] or in catalysis [5]. Undoped tin oxide film usually possesses higher resistance than doped one but this can be even an advantage in such application as transparent heating elements in aircraft and car windows for defogging and deicing purpose. SnO_2 thin films can be prepared by various methods such as the sol-gel technique [6], [7], reactive sputtering [8] spray pyrolysis [9] and chemical vapour deposition [10], [11]. The advantages of using the pyrolysis method are low equipment costs, good quality film produced over large substrate area with a very good adherence to the glass. Films can be deposited in an open atmosphere without sophisticated vacuum equipment. Economic advantage of the spray pyrolysis technique is especially important in production of large area films used in architectural and car windows. In this study tin oxide thin films were prepared by the spray pyrolysis technique using different precursors to establish the influence of the form of a precursor on the morphology and optical properties of the tin film.

2. Experimental procedure

The arrangement of the apparatus for the ultrasonic spray pyrolysis is shown in Fig. 1. An ultrasonic nebulizer operating at 44 kHz was used to produce mist with the droplet size smaller than 5 μm. Solution consumption was about 1 ml/min. Air was used as a gas carrier. Alcohol solutions of $SnCl_4$, $SnCl_2$ and $SnCl_2 \times H_2O$ (Aldrich) were used as a tin source. Composition of the solutions is shown in Tab. 1. The tin layers were deposited on the soda-lime microscope glass slides. Substrates were first cleaned with acetone in ultrasonic bath. Deposition temperature ranged from 400 to 600 °C and substrate temperature was controlled by Pt-PtRh thermocouple. Transmittance of the
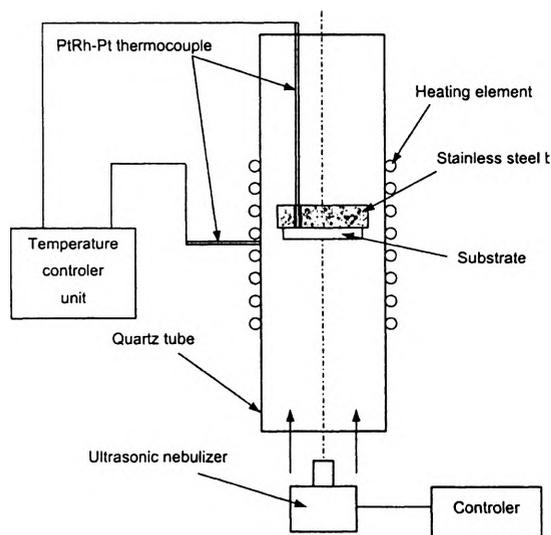

Fig. 1. Schematic drawing of the equipment arrangement used for thin film preparation by ultrasonic spray pyrolysis technique.

T a b l e 1. Chemical compositions of tin solutions.

Symbol	Composition
N01	$SnCl_4$ – 2.5 ml, methanol – 100 ml
N02	$SnCl_2 \times 2H_2O$ – 4.83 g, methanol – 100 ml
N03	$SnCl_2$ – 4.06 g, methanol – 100 ml
N04	$SnCl_4$ – 2.5 ml, methanol – 100 ml, H_2O (dest.) – 0.75 ml

tin film was measured by UV-VIS Hewlett–Packard 8453 spectrometer. X-ray photoelectron spectroscopy analyses were performed on "as made" samples using VSW spectrometer with a hemispherical analyser. Spectra were obtained using Al K_α radiation source operated at 200 W and 10 keV ($h\nu = 1486.6$ eV). The electron energy analyser was set to FAT mode with pass energy 22 eV. The shift of the binding energy

due to the surface charging effect was calibrated by assuming binding energy of C $1s$ to be always 284.6 eV. Depth profile was performed using EG10 argon gun operating at 2 keV. Impedance was measured at room temperature using HIOKI 3532 LCR meter. Microstructures of the coatings were observed with Joel 5400 scanning microscope.

3. Results and discussion

3.1. Optical properties

The transmittance curves of the SnO_2 films deposited at 550 °C during 5 min are shown in Fig. 2. All of the samples had high transparency (80–85%). The lowest transparency (~80%) was observed for the sample N03 because of high thickness of the film 402 nm, see Tab. 2. The thickness of the films was determined from interference maximum on the transmittance curves [12]. This method is applicable under following assumptions:

  – transmittance is measured under normal incidence,
  – there is little or no absorbance of the light in the film,
  – the film is uniform,
  – any edge effect can be neglected,
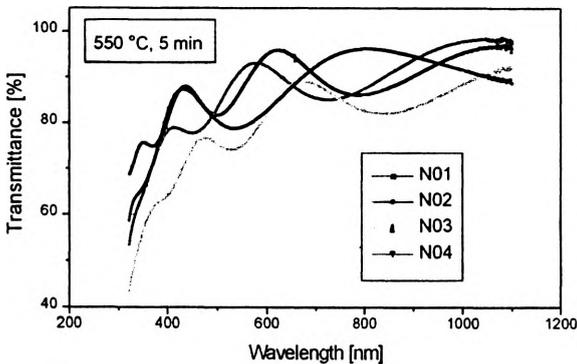 – refractive index is known (measured by another method) and is not wavelength dependent.

Fig. 2. Transmittance curves measured for samples deposited at 550 °C during 5 min.

T a b l e 2. Optical band gap, thickness and resistance of the tin films obtained at 550 °C, during 5 min deposition.

Symbol	d [nm]	E_{opt} [eV]	R [Ω/□]
N01	368	3.4	72
N02	370	3.5	65
N03	402	3.4	30
N04	233	3.1	105

M. Nocuń

Because the refractive index is usually wavelength dependent, it was assumed to be 2.0 at 550 nm [13] in this study. The thickness of the films has been calculated from the following relation [14]:

$$2nd = \left(\frac{1}{\lambda_1} - \frac{1}{\lambda_2}\right)^{-1} \tag{1}$$

where λ_1, λ_2 – the wavelengths at the successive maxima, n – the refractive index, d – the thickness of the film. The results were summarised in Tab. 2. The film growth rate as a function of deposition time for selected temperature (550 °C) is shown in Fig. 3. The lowest deposition rate was observed for sample N04 ($SnCl_4$ with water), while the highest deposition rate was obtained when $SnCl_2$ was used as a precursor (sample N03). Optical absorption coefficient α has been estimated from the equation [15]

$$\alpha(v) = \frac{1}{d} \ln \frac{1}{T(v)}. \tag{2}$$
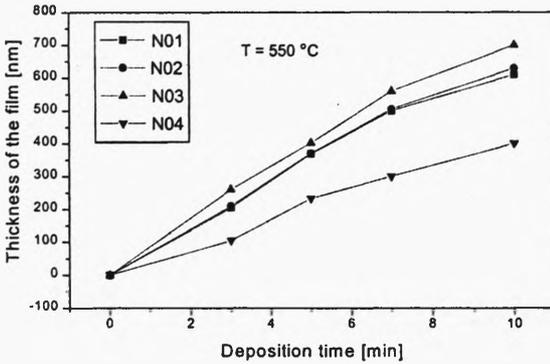

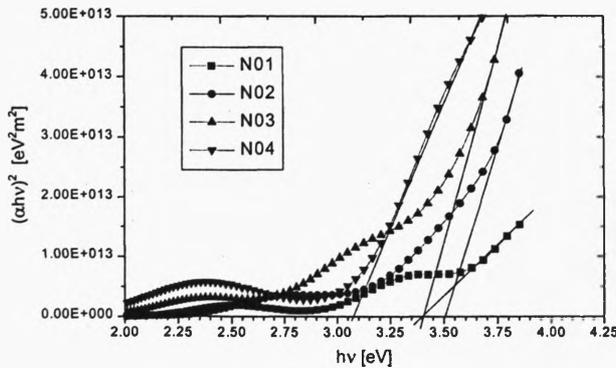Fig. 3. Rate of the film growth *vs.* deposition time. Sample prepared at 550 °C.

Fig. 4. Plots of $(\alpha h v)^2$ as a function of photon energy.

Using $\alpha(v)$ data optical band gap has been estimated from the relation

$$\alpha(v) = \frac{B(hv - E_{opt})^n}{hv} \tag{3}$$

where hv is the photon energy, B is the constant ($B = 10^5 - 10^6$ [16]), E_{opt} – the optical band gap energy, n – the exponent having value 1, 2, 3 or 0.5, depending on the electronic transition mechanism. $(\alpha hv)^2$ *vs.* hv relation for SnO_2 films obtained after 5 min deposition at 550 °C was shown in Fig. 4. Extrapolation of a straight-line region at high energy onto the x-axis gives value of the optical energy band gap, which is summarised in Tab. 2. The lowest value of optical band gap was measured for the sample N04 – 3.1 eV, while the highest value was observed for the sample N02 – 3.5 eV.

3.2. Photoelectron spectroscopy

In order to identify the chemical state of oxygen and tin in the deposited films X-ray photoelectron spectroscopy was carried out. Figure 5 shows a sequence of XPS spectra for O1s region. Spectrum 1 was measured for the sample without any preparation while spectra 2–4 were measured after sequential removing of the monolayers by ion sputtering (depth profiling technique). Two oxygen peaks with binding energies 530.5 and 532.5 eV are seen in Fig. 5. The first one, at 530.5 eV, is attributed to oxygen bonded to tin, and the second one comes from oxygen bonded to hydrogen (OH^- groups). High intensity of this peak suggests high sensitivity of the surface to the water vapour and
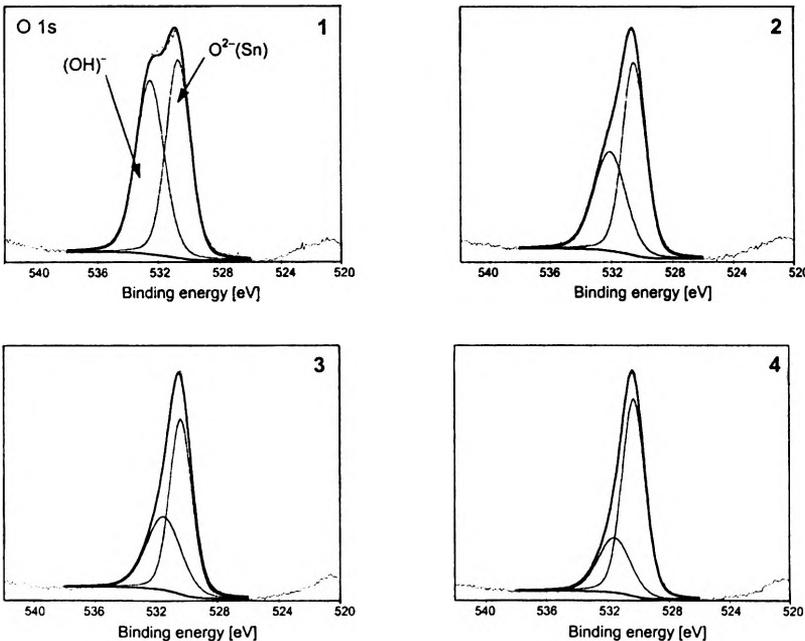

Fig. 5. XPS spectra of O 1s region. 1 – sample "as obtained", 2, 3, 4 – after subsequent sputtering.
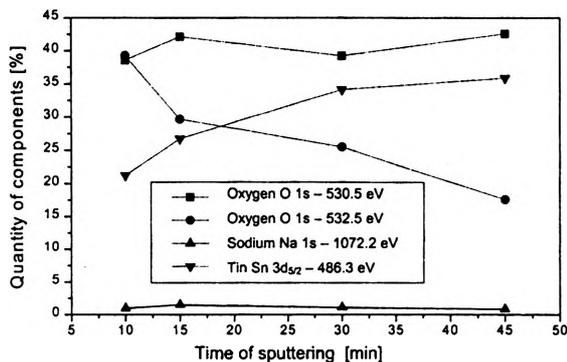
Fig. 6. Changes in the quantity of O 1s, Sn 3d$_{5/2}$ and Na 1s components as a function of sputtering time.
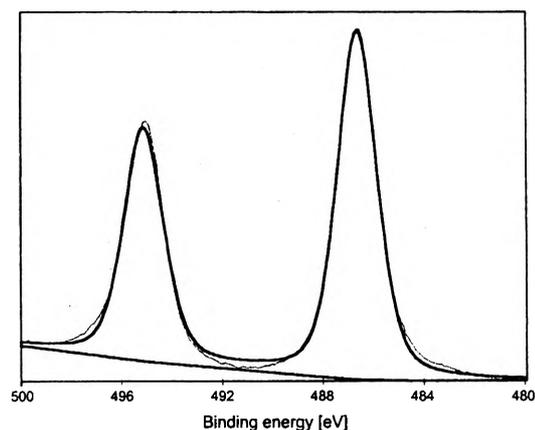

Fig. 7. Sn 3d region of the XPS spectra.

high surface area of the film. Subsequent sputtering leads to decrease in the intensity of this peak and to an increase in O 1s peak with binding energy 530.5 eV. Changes of Na 1s, O 1s and Sn 3d surface area after sputtering have been shown in Fig. 6. The intensity of O 1s peak, connected with water present at the surface, decreases with the time of sputtering, while the intensity of Sn 3d peak increases simultaneously. It confirms the fact that the surface is coverd with a layer of water. Some amount of sodium (about 1%) coming from glass substrate was also detected (Fig. 6). XPS spectrum of Sn 3d region reveals only one peak with Sn 3d$_{5/2}$ binding energy 486.6 eV (Fig. 7). Sputtering leads to lowering of this binding energy to the value 486.0 eV. It is a well -known fact that the Sn is hardly distinguishable from the XPS spectra. Binding energies from the range 486.2–486.7 eV (Sn 3d$_{5/2}$ peak) are usually attributed to Sn^{4+} [17], [18], and the energies from the range 485.6–486.0 eV to Sn^{2+} [19], [20]. Generally, higher value of binding energy is attributed to Sn^{4+}. In this study, tin exists in the film as a Sn^{4+} and observed lowering of the binding energy with the sputtering time was an effect of sputtering process, which led to the reduction of some Sn^{4+} atoms to Sn^{2+}.

3.3. Microstructure observations

SEM picture of the tin surface reveals crystalline texture with a uniform crystal size
(0.1–0.5 μm) and uniform distribution at the surface (Fig. 8). However, morphology
of the films obtained from $SnCl_2$ precursor differs from the morphology of the films
obtained from $SnCl_4$ precursor. SnO_2 films obtained from $SnCl_2$ and $SnCl_2×2H_2O$
demonstrate a crystalline structure, with higher roughness and with sharp grain
crystals. Porosity of the films is much lower as compared to the films obtained from
$SnCl_4$ (Fig. 8b and c). $SnCl_4$ precursor gives much smoother surface, still crystalline
but with much smaller crystals (Fig. 8a and d). High pores (~1 μm), sometimes with
a regular shape, were observed in case of sample N01. Sample N04, when $SnCl_4$ was
used as a precursor and in the presence of water, exhibits much higher porosity. This
porosity is most probably due to large water droplet evaporation during the pyrolysis
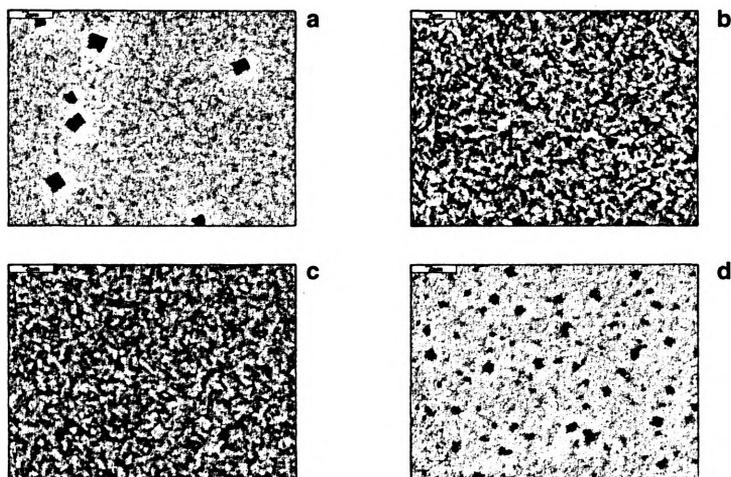process.

Fig. 8. SEM images of tin layers obtained from different precursors: $SnCl_4$ (a), $SnCl_2×2H_2O$ (b), $SnCl_2$ (c),
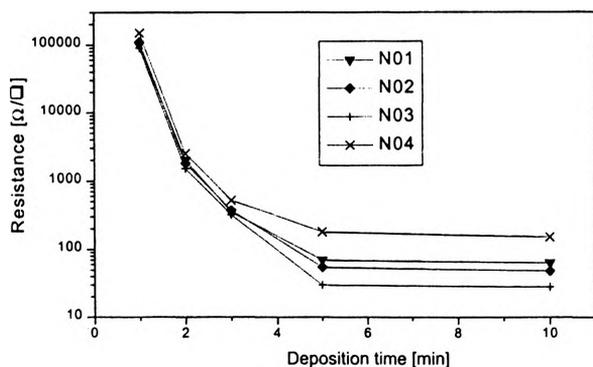$SnCl_4$ + H_2O (d).

Fig. 9. Surface resistance *vs.* deposition time.

3.4. Resistance measurement

Resistance of the films was measured using 2 electrodes system. Selected results were shown in Fig. 9 and collected in Tab. 2. Resistance of the samples correlates with the thickness of the film. The lowest value of resistance was measured for the sample N03 with a thick layer of SnO_2, while resistance of the sample N04 was much higher (Tab. 2).

4. Conclusions

Physical properties of the tin films obtained by the spray pyrolysis method strongly depend on the form of a precursor. $SnCl_2$ leads to a higher rate of film formation and produces low resistivity and low porosity high crystalline film. Precursor in the form of $SnCl_4$ gives a smooth SnO_2 film with comparable resistivity but much higher porosity, especially in the case when water is present in the solution. In all studied samples, tin was present in the form of Sn^{4+}.

References

[1] CHOPRA K.L., MAJOR S., PANDYA K., Thin Solid Films 102 (1983), 1.
[2] BUCHER E., Appl. Phys. 17 (1978), 1.
[3] HE Y.S., CAMPBELL J.C., MURPHY R.C., ARENDT M.F., SWINNEA J.S., J. Mater. Res. 8 (1993), 3131.
[4] NITTA M., OHTANI S., HARDOME M., J. Electron. Mater. 9 (1980), 727.
[5] BERRY F.J., Adv. Catalysis 30 (1982), 97.
[6] CHATELON J.P., TERRIER C., BERNSTEIN E., BERJOAN R., ROGER J.A., Thin Solid Films 247 (1994), 162.
[7] PARK S.S., MACKENZIE J.D., Thin Solid Films 258 (1995), 268.
[8] SINCLAIR W.R., PETERS F.L., STILLINGER D.W., KOONCE S.E., J. Electrochem. Soc. 112 (1965), 1096.
[9] SHANTHI E., DUTTA V., BANERJEE A., CHOPRA K.L., J. Appl. Phys. 51 (1980), 6243.
[10] MARUYAMA T., MORISHITA T., Thin Solid Films 251 (1994), 19.
[11] ABOAF J.A., MARCOTTE V.C., CHOU N.J., J. Electrochem. Soc. 120 (1973), 701.
[12] CISNEROS J.I., REGO G.B., TOMYIAMA M., BILAC S., GONCALVES J.M., RODRIGUEZ A.E., ARGUELLO Z.P., Thin Solid Films 100 (1983), 155.
[13] DARAZOGLON D., Thin Solid Films 302 (1997), 204.
[14] MANIFACIER J.C., GASIOT J., FILLARD J.P., J. Phys. E 9 (1976), 1002.
[15] McGUIRE G.E., SCHWEITZER G.K.K., CARLSON T.A., Inorg. Chem. 12 (1973), 2451.
[16] DAVIS E.A., MOTT N.F., Philos. Mag. 22 (1970), 903.
[17] HASHEMI T., HOGARTH C.A., GOLESTANI-FARD F., J. Mater. Sci. 23 (1988), 2645.
[18] GRUTSCH P.A., ZELLER M.V., FEHLNER T.P., Inorg. Chem. 12 (1973), 1432.
[19] SHUTTLEWORTH D., J. Phys. Chem. 84 (1980), 1629.
[20] ANSELL R.O., DICKINSON T., POWEY A.F., SHERWOOD P.M.A., J. Electron Spectrosc. Relat. Phenom. 11 (1977), 301.